Limitation Analysis of 1st and 2nd Generation Superconductors used in Resistive Superconductor Fault Current Limiters

Buğra Yılmaz[*], Muhsin Tunay Gençoğlu[**]

[*]Department of Aviation Electrical Electronics, School of Civil Aviation, Firat University, Elazig, 23100, Turkey.

[**]Department of Electrical and Electronics Engineering, Faculty of Engineering, Firat University, Elazig, 23100, Turkey.

[*]Corresponding Author: b.yilmaz@firat.edu.tr

ABSTRACT

Fault currents in power systems force valuable power system elements thermally, dynamically, and electromagnetically until the arc disappears. Installation elements that can withstand fault currents or damage existing components require a high cost. Installing components that withstand fault currents and the damage of fault currents to existing components are costly. Resistive Superconducting Fault Current Limiter (R-SFCL), one of the modern limiting methods, increases the safety and sustainability of the system by eliminating these risks. In this study, a dynamic model was created in MATLAB/Simulink for 1G and 2G HTS used in R-SFCL, and their response to single phase-to-ground fault was observed. According to the simulation results, the most advantageous HTS type for R-SFCL was determined. The fault current level, limitation rate, resistance and temperature values, and response times were compared in terms of limiting performance.

Keywords: Dynamic simulation; Fault current limitation; MATLAB/Simulink; Resistive SFCL; Superconductor.

INTRODUCTION

The increasing world population and industrialization have increased energy demand in recent years. New electricity generation, transmission, and distribution systems are added to existing systems to meet the growing demand for electrical energy. While the increase in production capacity increases the levels of short-circuit currents, the spread of the interconnected system over large areas increases the probability of fault. Power system fault currents reach 5 to 20 times the nominal current (Leung, 2009). High-level fault currents can cause irreversible damage to the system and its components. Therefore, power system breakers have to trip the fault current as soon as possible. This causes the breaker to face a larger fault current due to the effect of the DC factor of the fault current. Considering that the tripping capability of typical high voltage breakers is limited to 80 kA, rising levels of fault currents will soon exceed the capabilities of existing breakers (Seyedi & Tabei, 2012). The typical breakers' capabilities were about 40 kA in the 1990s and 63 kA in the 2000s (Moyzykh et al., 2021). In 2013, an 80 kA gas-insulated breaker was installed in New Jersey, USA (Labos & Grossmann, 2014). Higher tripping capacity will increase both size and cost. Because of these situations, the fault current needs to be reduced quickly to non-hazardous levels.

Many methods have been developed to limit the current (Saha et al., 2019). Although series reactors added to the circuit limit the current, they increase the voltage drop under normal operating conditions. While fuses called Is-limiters do not cause power loss in normal conditions, replacing the fuse after each short circuit is necessary. (Kempski et al., 2019). Superconducting Fault Current Limiters (SFCL), one of the modern fault current limiting methods, offer an attractive solution to fault currents (Blair et al., 2012) (Barzegar-Bafrooei et al., 2019). Elimination of the mentioned disadvantages is possible by using SFCLs, which use the abrupt transition of superconducting material from superconducting to the resistive region at a specific critical current value (Nagarathna et al., 2015) (X. Chen et al., 2022) (Zampa et al., 2022). SFCLs are the best alternative to replace conventional limiting methods thanks to the advantages of superconducting materials (J. Lee & Joo, 2013). They produce a low voltage drop and power loss at nominal current (J. Zhang et al., 2019). If the critical values such as critical temperature (T_c), critical current density (J_c), or critical magnetic field (H_c) are exceeded, the resistance of the superconductor will increase. (X. Zhang et al., 2015). Then the short circuit ends, and SFCL cools down and returns to the superconducting region. SFCL is usually disconnected from the network during cool down by a circuit breaker (Gorbunova et al., 2020). SFCL, whose applications have become widespread thanks to its protection, can be classified

into two types. These are Resistive SFCL and Inductive SFCL. Resistive SFCL (R-SFCL) is the most promising method due to its small size and decreasing superconductor prices (Jiahui Zhu et al., 2019). R-SFCL reduces the influence of the DC factor of the fault current by lowering the X/R ratio. It does not cause harmonic and magnetic field interference.

For this reason, recently, R-SFCL applications have been more preferred in power systems (Jiahui Zhu et al., 2020) (S. R. Lee et al., 2017). Many superconducting materials are used in the R-SFCL design. Superconductors are divided into two groups according to their temperature: High-Temperature Superconductors (HTS) and Low-Temperature Superconductors (LTS). The HTS is cooled with liquid Nitrogen (LN_2) and has a critical temperature of over 30 °K. This is a massive advantage over LTS materials, which operate at 4.2 °K, are very close to their critical temperature, and are very sensitive to temperature changes. SFCL based on LTS could not be commercialized because it required a costly cooling system using liquid Helium (LHe) (Okakwu et al., 2018). When using HTS for SFCL applications, cooling costs can be reduced ten times instead of LTS (Zenitani & Akimitsu, 2002). HTS materials can also be classified as 1G and 2G. 2G HTS materials have higher current carrying capacity, critical current level, magnetic flux value, and mechanical strength (Yılmaz & Gençoğlu, 2022). In addition, 2G materials pass into the resistive region faster than 1G materials (Kim & Kim, 2011). Likewise, after the fault is complete, the 1G HTS returns to the superconducting region later than the 2G HTS and 1G HTS has a lower normal operation resistance than 2G HTS (Kulkarni et al., 2012) (Jiamin Zhu et al., 2022). This paper describes the limitation analysis of 1G and 2G HTS materials used in the R-SFCL structure by creating a dynamic model in MATLAB/Simulink. The simulation results were evaluated for 1G and 2G HTS materials.

MODELING AND SIMULATION OF RESISTIVE SFCL

The current through the R-SFCL is less than the critical current value during normal operating conditions. Therefore, the resistance is close to zero, and the R-SFCL conducts electricity almost without loss. However, in the event of a fault, the current exceeds the critical current value, and the resistance of the superconducting material increases. Thus, the R-SFCL limits the fault current (Moyzykh et al., 2021). Briefly, R-SFCL, which produces a negligible voltage drop and power loss in normal operation, limits the fault current level with a nonlinear increase in resistance within the first half-period when the fault occurs. The discovery of HTS has enabled the production of various superconducting materials in the laboratory environment. Some superconducting materials used in the R-SFCL structure are given below:

- YBa$_2$Cu$_3$O$_7$ (Yttrium Barium Copper Oxide-YBCO, T$_c$=92 °K, 2G HTS)
- GdBa$_2$Cu$_3$O$_7$ (Gadolinium Barium Copper Oxide-GdBCO, T$_c$=91 °K, 2G HTS)
- Bi$_2$Sr$_2$CaCu$_2$O$_8$ (Bismuth Strontium Calcium Copper-BSCCO 2212 or Bi2212, T$_c$=95 °K, 1G HTS)
- Bi$_2$Sr$_2$Ca$_2$Cu$_3$O$_{10}$ (BSCCO 2223 or Bi2223, T$_c$=107 °K, 1G HTS)
- MgB$_2$ (Magnesium Diboride, T$_c$=39 °K, 2G HTS) (List of Superconductors, n.d.).

The R-SFCL model is based on the E-J characteristic curve shown in Figure 1. The instantaneous variation of the R-SFCL resistance is also based on the relationship between the electric field (E) and the current density (J) (Hatata et al., 2018) (De Sousa et al., 2014) (Y. Chen et al., 2013). This curve has three possible superconducting material regions: superconducting, flux-flow, and resistive (normal) region.
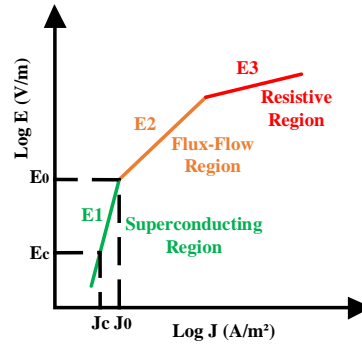

Figure 1. E-J characteristic curve

The resistance and current density of the R-SFCL for all regions are calculated by the following equations (Blair et al., 2012) (X. Zhang et al., 2015) (Hatata et al., 2018) (Nemdili & Belkhiat, 2012) (Aly & Mohamed, 2012) (Xue et al., 2015).

$$R_{Rsfcl}(t) = \frac{E(J,T)\ L_s}{J(t)\ A_s} \tag{1}$$

$$J(t) = \frac{I_{Rsfcl}(t)}{A_s} \tag{2}$$

where R$_{Rsfcl}$ is the instant R-SFCL resistance (Ω), L$_s$ is the superconductor length (m), A$_s$ is the superconductor section (m^2), E is the electric field as a function of J and T (V/m), T is the instant R-SFCL temperature (°K), I$_{Rsfcl}$ is the instant R-SFCL current (A), and J is the instant current density (A/m^2).

Superconducting Region

The R-SFCL current is below the critical value, and the R-SFCL resistance is approximately

zero. E is calculated by the formula below (Blair et al., 2012) (Nemdili & Belkhiat, 2012) (Dutta & Babu, 2014).

$$E(J,T) = E_c \left(\frac{J}{J_c(T)}\right)^{\alpha} \tag{3}$$

$$J_c(T) = J_c \left(\frac{T_c - T}{T_c - T_0}\right) \tag{4}$$

$$\alpha_x = \frac{\log\left(E_0/E_c\right)}{\log\left(\left(J_c/J_c(T)\right)^{\left(1-\frac{1}{\beta}\right)} \left(E_0/E_c\right)^{\frac{1}{\alpha}}\right)} \tag{5}$$

$$\alpha = \max[\beta, \alpha_x] \tag{6}$$

where E_c is the critical electric field (1 µV/cm), J_c (T) is the critical current density (A/m^2) as a function of T, J_c is the critical current density at 77 °K, T_c is the critical temperature (°K), T_0 is the first temperature value (77 °K), α_x is the time-varying value of the exponential value, α is the superconducting region exponent value, the α value ranges from 5-15 for 1G HTS materials and 15-40 for 2G HTS materials (Dutta & Babu, 2014) (Qian et al., 2017) (Manohar & Ahmed, 2012).

Flux-Flow Region

Exceeding the critical current increases the R-SFCL resistance as the electric field increases and the current is limited. The temperature rises, and the rising temperature lowers J_c(T), so the electric field increases continuously. E is calculated by the formula given below (X. Zhang et al., 2015) (Nemdili & Belkhiat, 2012) (Xue et al., 2015).

$$E(J,T) = E_0 \cdot \left(E_c/E_0\right)^{\beta/\alpha} \frac{J_c}{J_c(T)} \left(J/J_c\right)^{\beta} \tag{7}$$

E_0 is the electric field during the transition from the superconducting region to the flux-flow region (V/m) and takes a value between 0.1 and 1 V/m, β is the exponent of the flux-flow region for both 1G and 2G HTS materials ranging from 2-4 (Dutta & Babu, 2014) (Qian et al., 2017) (Manohar & Ahmed, 2012).

Resistive (Normal) Region

As soon as the temperature exceeds the critical temperature, R-SFCL is no longer superconducting. R-SFCL resistance and E vary with J and T. E is calculated by the formula given below (X. Zhang et al., 2015) (Nemdili & Belkhiat, 2012) (Xue et al., 2015).

$$E(J,T) = \rho(T_c) J \frac{T}{T_c} \tag{8}$$

where $\rho(T_c)$ is the superconductor resistivity in the resistive region ($\Omega.m$).

During this process, the superconducting material heats up. After recovery, the cryogenic system cools the superconducting material and returns to the R-SFCL superconducting region.

Thermal Calculations

The heat transfers between LN$_2$ and superconducting material and R-SFCL temperature variations are calculated with the formulas given below (Blair et al., 2012) (X. Zhang et al., 2015) (Nemdili & Belkhiat, 2012)(Xue et al., 2015) (Elmitwally, 2009) (Langston et al., 2005) (Liang et al., 2022). The R-SFCL resistance will increase when the fault current exceeds the critical current level. This increase will cause its temperature to increase with the I^2R formula. The superconducting material will need to be well cooled to avoid a Hot-Spot. The heat energy that the liquid nitrogen removes from the heated superconductor is calculated according to Equation 11, and the new temperature is calculated for each iteration according to the heat capacity of the superconductor. The heat capacity of the superconductor depends on its length, cross-sectional area, and volumetric specific heat. R-SFCL temperature has been calculated at the end of the simulation period with the interaction between the generated and received heat.

$$Q_{Rsfcl}(t) = \int I_{Rsfcl}(t)^2 \, R_{Rsfcl}(t) \, dt \tag{9}$$

$$Q_{cryosys}(t) = \int \left(\frac{T(t)-T_0}{\theta_s} \right) dt \tag{10}$$

$$\theta_s = \frac{1}{k \, L_s \, \pi \, d_s} \tag{11}$$

$$T_{Rsfcl} = T_{Rsfcl} + (Q_{Rsfcl} - Q_{cyrosys})/c_s \tag{12}$$

$$c_s = L_s \, A_s \, c_{vol} \tag{13}$$

where Q_{Rsfcl} is the heat energy emitted by the R-SFCL (J), $Q_{cryosys}$ is the heat energy received by the cryogenic system (J), θ_s is the thermal resistance between R-SFCL and cryogenic system (K/W), k is the heat transfer coefficient to the cryogenic system (W/Km^2), d_s is the

superconductor diameter (m), c_s is the superconductor heat capacity (J/K), c_{vol} is the superconductor volumetric specific heat (J/Km^3), T_{Rsfcl} is the R-SFCL instant temperature (°K). All formulas have been modeled as M-function in MATLAB/Simulink according to parameters in Table 1. The simulation system is shown in Figure 2, the dynamic modeling algorithm given in Figure 3, and Figure 4 (a) shows the MATLAB/Simulink model of the power system with R-SFCL, Figure 4 (b) shows the subsystem of R-SFCL. R-SFCLs typically contain an impedance parallel to the R-SFCL (Blair et al., 2011). To simplify the analysis in this article, shunt impedance is assumed to be absent. The shunt impedance affects the recovery time of the R-SFCL and does not affect the following section's analysis (Blair et al., 2012). Various faults occur in power systems (Nejra et al., 2019). This study investigated single phase-to-ground fault, the most common fault type at medium voltage levels (Ahmadi et al., 2021).

Table 1. Parameters of simulation

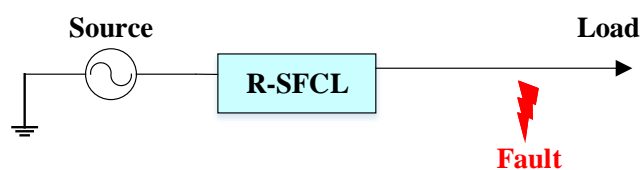| Parameters	Value	Parameters	Value
Source Voltage	11 kV	c_{vol}	1 x 10^6 J/K.m^3
Short Circuit Level	50 MVA	α for 1G HTS	10
X/R	7	α for 2G HTS	35
Load	10 MW, 8 MVAr	β	4
R-SFCL Critical Current ($I_{c77°K}$)	560.46 A$_{rms}$	d_s	0.004 m
ρ(T_c) for 1G HTS	1 x 10^{-6} Ω.m	T_0	77 °K
ρ(T_c) for 2G HTS	5 x 10^{-6} Ω.m	T_c for 1G HTS	105 °K
E_c	1μ V/cm	T_c for 2G HTS	95 °K
E_0	0.1 V/m	T_s (Step Time)	1 x 10^{-5} s
k	1.5 x 10^3 W/K.m^2	Superconductor Length	150 m

Figure 2. Simulation system
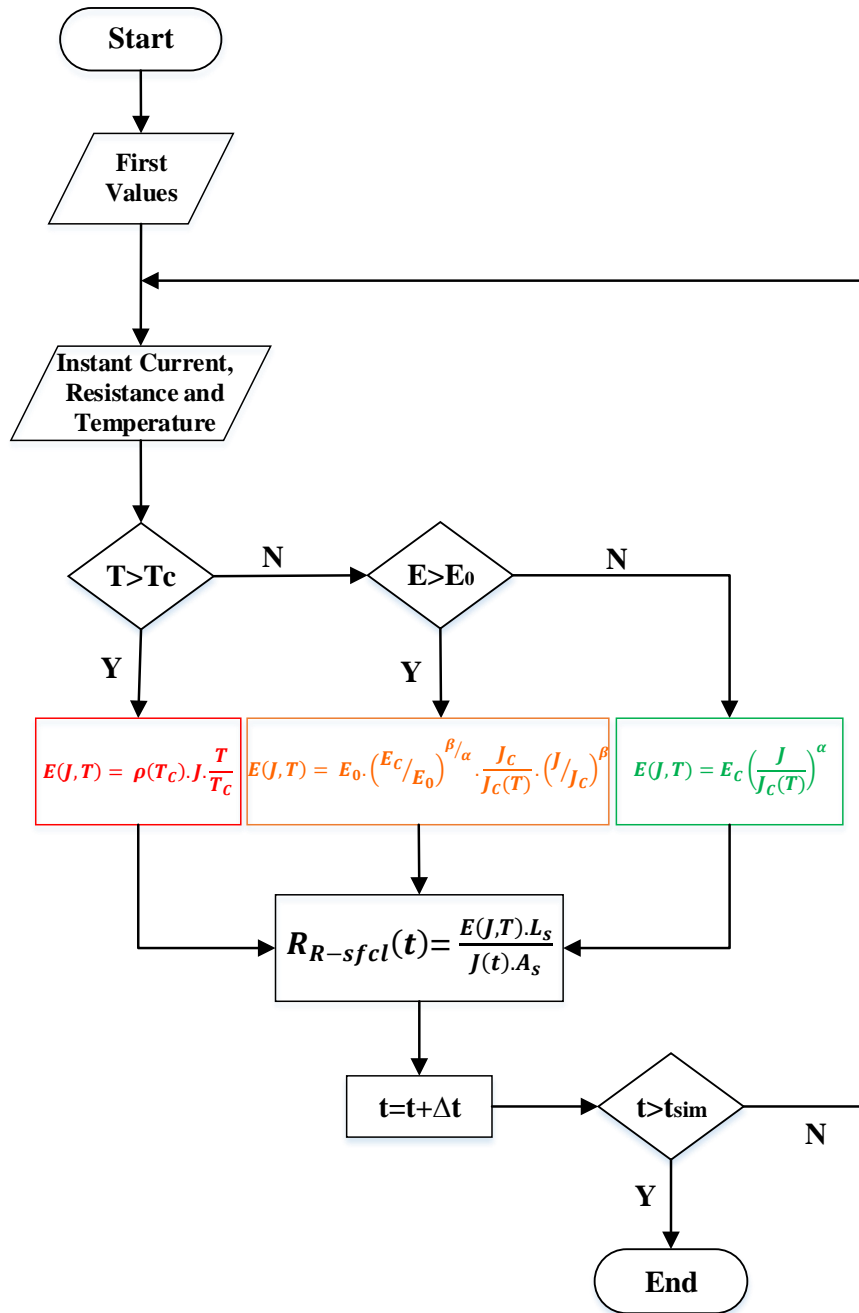
Figure 3. Dynamic modeling algorithm of R-SFCL
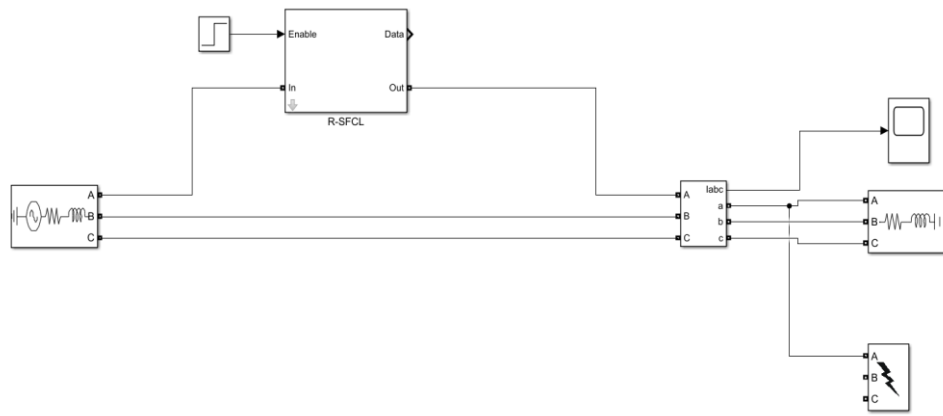
(a)
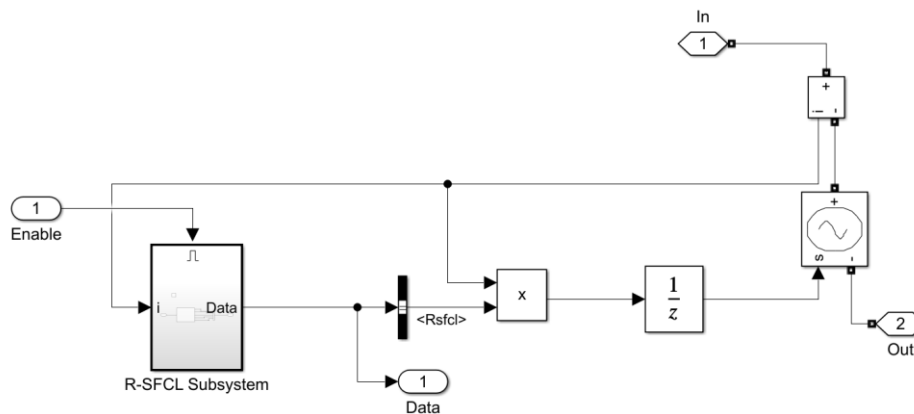
(b)

Figure 4. (a) MATLAB/Simulink model of the power system with R-SFCL **(b)** R-SFCL subsystem

In the R-SFCL design, the superconducting material can be coil differently. Examples of these connections are zigzag, inductive, and non-inductive bifilar coil connections. Each HTS module is wrapped according to one of these winding types. In this study, modeling has been done for non-inductive bifilar coil winding. Depending on where the R-SFCL is installed, the HTS modules are connected in series as the voltage level increases. Conversely, they are connected in parallel as the current level increases. Sometimes kilometers of superconductors are required, depending on the voltage and current level. For example, in the 220 kV 1200 A SFCL application, a 25 km long superconductor is used for three phases (Moyzykh et al., 2021). Another essential point in R-SFCL design is the cryogenic system. Generally, closed-loop cooling systems that provide liquid nitrogen circulation at high pressure are preferred. Since almost all of the energy consumed by R-SFCL under normal operating conditions is sourced from the cryogenic system, the elements of this system such as tank, valves, pipelines, and pump should be carefully selected.

Besides its advantages, R-SFCL has some disadvantages, including the investment cost. Today, the expensiveness of superconducting materials and the cryogenic system makes it difficult for R-SFCL applications to be applied outside certain developed countries. Another negative aspect is the need for constant cryogenic fluid maintenance. As a result, the R-SFCL with its cryogenic system will occupy the same volume as an average power transformer. Some manufacturers also produce R-SFCL, which covers an area of a few square meters according to the voltage and current level.

RESULT AND DISCUSSION

This section examined the limitation performance of 1G and 2G HTS materials used in the R-SFCL structure and their response to the fault. First, simulations were made for 1G HTS material and 2G HTS material with the parameters in Table 1. It lasts as long as the average opening time of typical breakers (60 milliseconds). The critical current is close to the nominal current but slightly higher. Figure 5 shows the fault current occurring in the system without R-SFCL.
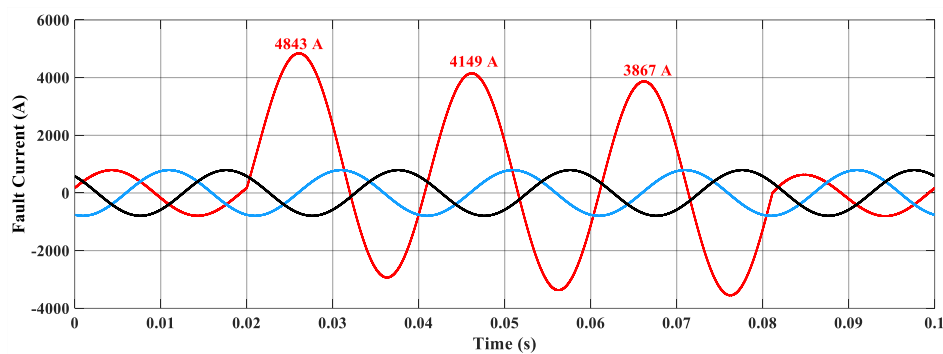

Figure 5. Fault current without R-SFCL

The fault current of the system with R-SFCL designed with 1G HTS is in Figure 6.
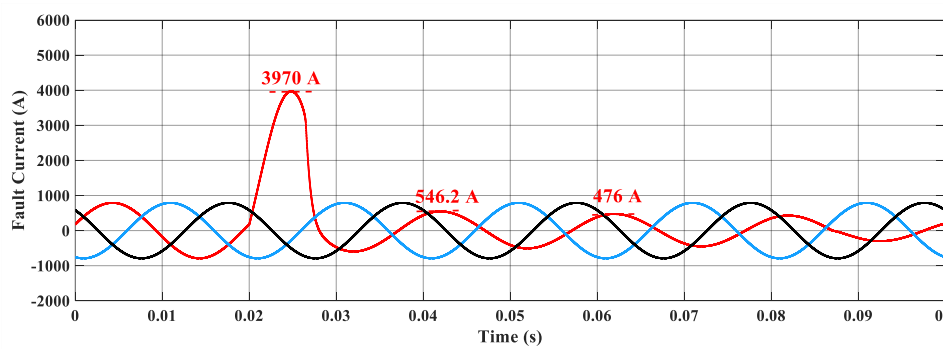

Figure 6. Fault current with 1G HTS R-SFCL

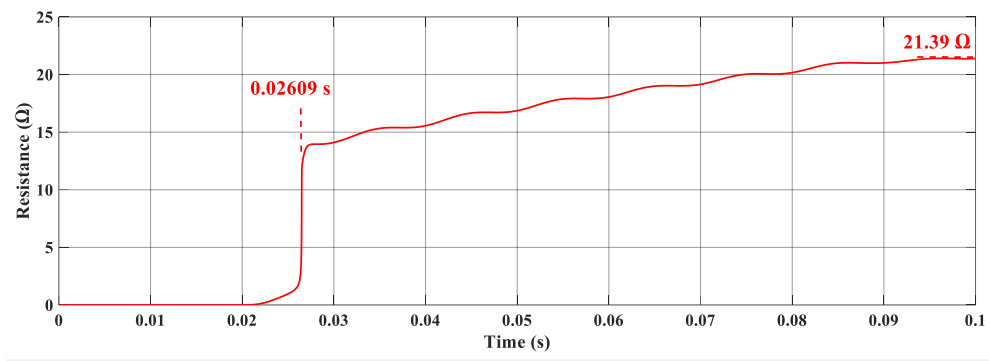Figure 7 and Figure 8 show the resistance and temperature variation of this R-SFCL during the fault, respectively.

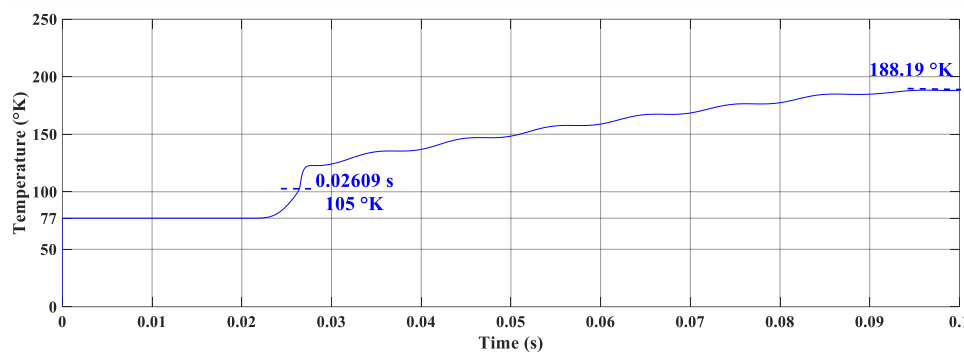**Figure 7.** Resistance variation of 1G HTS R-SFCL

Figure 8. Temperature variation of 1G HTS R-SFCL

After 1G HTS, simulations were carried out for 2G HTS with the same length. Figure 9 shows the fault current of the system with R-SFCL designed with 2G HTS.
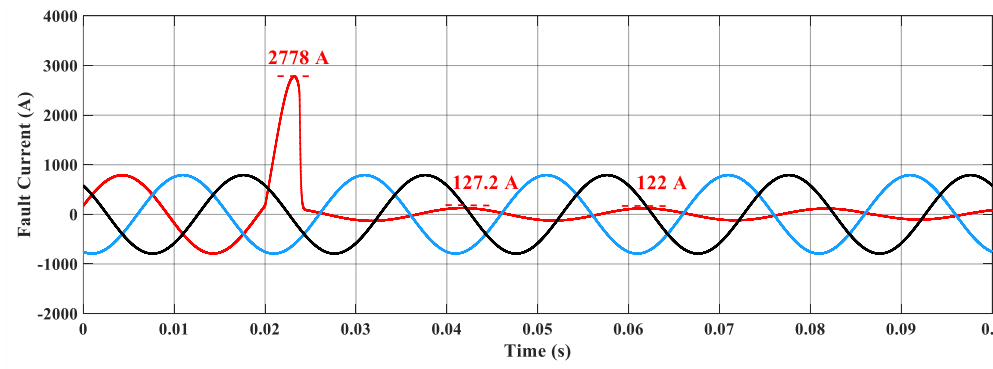

Figure 9. Fault current with 2G HTS R-SFCL

The resistance and temperature variations of R-SFCL using 2G HTS are given in Figure 10 and Figure 11, respectively.
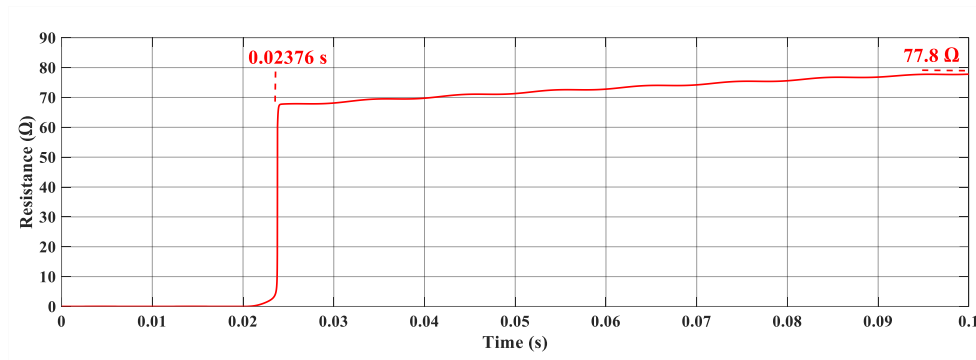
11

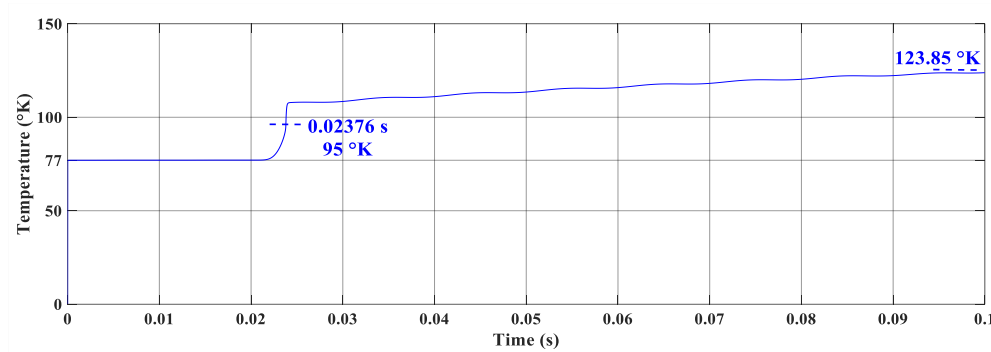**Figure 10.** Resistance variation of 2G HTS R-SFCL

Figure 11. Temperature variation of 2G HTS R-SFCL

The simulation results show that R-SFCL has considerably limited the fault current regardless of 1G or 2G HTS. This limitation process was carried out within the first half-period after the fault occurred and continued until the end of the fault. Response times to fault are 6.09 milliseconds for 1G HTS R-SFCL and 3.76 milliseconds for 2G HTS R-SFCL, respectively. As stated in the literature, 2G HTS transitioned to the resistive region faster than 1G HTS. At the same time, the 2G HTS has a higher resistance value than the 1G HTS for the same length and has better limited the first peak of the fault. Therefore, a more extended 1G HTS is required to achieve the same limiting performance.

As the superconductor length increases, an inhomogeneous I_c distribution on the surface also increases so that the Hot-Spot event may be inevitable. It is seen that 1G HTS heats more than 2G HTS during fault. Based on this, it can be concluded that the recovery time required after a fault may be longer for 1G HTS. Prolonged recovery time leads to unnecessary power loss and voltage drop in normal operating conditions like conventional limitation methods (reactor, high impedance transformer, etc.). Therefore, shortening the recovery time is an important goal for R-SFCL manufacturers. The topic of shortening the recovery time will be examined in future studies. The comparison of simulation results is given in Table 2.

Table 2. Limitation comparison

	w/o R-SFCL	w/ 1G HTS R-SFCL	w/ 2G HTS R-SFCL
Limiting Rate at First Peak Current (%)	-	18.03	42.64
Fault Resistance (Ω)	-	21.39 Ω	77.8 Ω
Fault Temperature (°K)	-	188.19 °K	123.85 °K

The modeling and simulations performed in this study were compared in Table 3 with other published articles that did similar work. In this study, the model made for 1G HTS is Model 1, and the model made for 2G HTS is Model 2. The voltage and short-circuit power levels of the simulation systems in which these models are applied are different. At the same time, the superconductor length and resistivity (ρ) also vary according to the study.

Table 3. Modeling comparison

	HTS Element	Resistance (Ω)	Temperature (°K)	First Peak Limiting Ratio (%)
Model 1	1G	21.39	188.19	18.03
Model 2	2G	77.8	123.85	42.64
(Aly & Mohamed, 2012)	1G	2.3	125	≈55
	2G	15-20	200-250	≈60
(Nemdili & Belkhiat, 2012)	1G	-	-	83.4
(X. Zhang et al., 2015)	1G	5	275	35
(De Sousa et al., 2016)	2G	5-6	90-95	84.25
(Jiahui Zhu et al., 2015)	2G	-	-	33.3
(Blair et al., 2012)	1G	≈20	400-450	-
(Hatata et al., 2018)	1G	10-15	-	52.5

As seen in Table 3, there are different resistance, temperature, and limiting ratio results for different HTS types. The main reason for this difference is that many parameters can be taken approximately but still differently while modeling. As a result, the models in this study are consistent with the literature average.

CONCLUSION

Fault current limitation has become inevitable as the growth of power systems increases fault current levels. Various superconductors are used in the R-SFCL structure, eliminating conventional methods with their advantages. This paper examines the response of R-SFCLs using 1G and 2G HTS to fault current. The dynamic model based on the E-J curve is created in MATLAB/Simulink for 1G and 2G HTS. As simulation results, fault currents, R-SFCL resistance, and temperature values are obtained. It has been observed that the 2G HTS R-SFCL reduces the initial peak value of the fault current by approximately half in the power system model. In addition, as seen in the resistance graphs, 2G HTS shows a faster response and higher resistance value, which is more advantageous than 1G HTS in terms of R-SFCL.

On the other hand, the lower fault temperature value makes the 2G HTS less thermally stressed. In the light of the results, using 2G HTS in R-SFCL designs will provide a more efficient and reliable limitation process. Although R-SFCL's need for a cryogenic system and expensive superconductors is considered a disadvantage, it does not cause power loss/voltage drop in normal operating conditions. It has an effective limitation process, making its applications widespread in recent years. Since the increase in demand for superconductors will increase production, superconductor prices will decrease to affordable levels, making R-SFCL more popular.

RECOMMENDED FUTURE WORKS

In this study, only limitation analysis was performed for R-SFCL. The model aiming to shorten the recovery time after the fault will be examined in future studies.

REFERENCES

Ahmadi, A., Aghajari, E., & Zangeneh, M. (2021). Earth fault detection in distributed power systems on the basis of artificial neural networks approach. *Journal of Engineering Research*, 1–17. https://doi.org/10.36909/jer.13627

Aly, M. M., & Mohamed, E. A. (2012). Comparison between resistive and inductive superconducting fault current limiters for fault current limiting. *Proceedings - ICCES 2012: 2012 International Conference on Computer Engineering and Systems*, 227–232. https://doi.org/10.1109/ICCES.2012.6408518

Barzegar-Bafrooei, M. R., Foroud, A. A., Ashkezari, J. D., & Niasati, M. (2019). On the advance of SFCL: A comprehensive review. *IET Generation, Transmission and Distribution*, *13*(17), 3745–3759. https://doi.org/10.1049/iet-gtd.2018.6842

Blair, S. M., Booth, C. D., & Burt, G. M. (2012). Current-time characteristics of resistive superconducting fault current limiters. *IEEE Transactions on Applied Superconductivity*, *22*(2), 5600205. https://doi.org/10.1109/TASC.2012.2187291

Blair, S. M., Member, S., Booth, C. D., Singh, N. K., Burt, G. M., & Bright, C. G. (2011). Analysis of Energy Dissipation in Resistive Superconducting Fault-Current Limiters for Optimal Power System Performance. *IEEE Transactions on Applied Superconductivity*, *21*(4), 3452–3457. https://doi.org/10.1109/TASC.2011.2129518

Chen, X., Zhang, M., Chen, Y., Jiang, S., Gou, H., Lei, Y., & Shen, B. (2022). Superconducting fault current limiter (SFCL) for fail-safe DC-DC conversion: From power electronic device to micro grid protection. *Superconductivity*, *1*(March), 100003. https://doi.org/10.1016/j.supcon.2022.100003

Chen, Y., Li, S., Sheng, J., Jin, Z., Hong, Z., & Gu, J. (2013). Experimental and numerical study of co-ordination of resistive-type superconductor fault current limiter and relay protection. *Journal of Superconductivity and Novel Magnetism*, *26*(11), 3225–3230. https://doi.org/10.1007/s10948-013-2181-9

De Sousa, W. T.B., Polasek, A., Dias, R., Matt, C. F. T., & De Andrade, R. (2014). Thermal-electrical analogy for simulations of superconducting fault current limiters. *Cryogenics*, *62*, 97–109. https://doi.org/10.1016/j.cryogenics.2014.04.015

De Sousa, Wescley Tiago Batista, Assis, T. M. L., Polasek, A., Monteiro, A. M., & De Andrade, R. (2016). Simulation of a superconducting fault current limiter: A case study in the Brazilian power system with possible recovery under load. *IEEE Transactions on Applied Superconductivity*, *26*(2). https://doi.org/10.1109/TASC.2015.2510609

Dutta, S., & Babu, B. C. (2014). Modelling and analysis of resistive Superconducting Fault Current Limiter. *IEEE TechSym 2014 - 2014 IEEE Students' Technology Symposium*, 362–366. https://doi.org/10.1109/TechSym.2014.6808076

Elmitwally, A. (2009). Proposed hybrid superconducting fault current limiter for distribution systems. *International Journal of Electrical Power and Energy Systems*, *31*(10), 619–625. https://doi.org/10.1016/j.ijepes.2009.06.002

Gorbunova, D. A., Kumarov, D. R., Scherbakov, V. I., Sim, K., & Hwang, S. (2020). Influence of polymer coating on SFCL recovery under load. *Progress in Superconductivity and Cryogenics (PSAC)*, *12*(1), 44–47. https://doi.org/10.9714/psac.2019.21.4.044

Hatata, A. Y., Ebeid, A. S., & El-Saadawi, M. M. (2018). Application of resistive super conductor fault current limiter for protection of grid-connected DGs. *Alexandria Engineering Journal*, *57*(4), 4229–4241. https://doi.org/10.1016/j.aej.2018.11.009

Kempski, A., Rusinski, J., & Hajdasz, S. (2019). Analysis of Recovery Time of HTS Tapes with Electrical Insulation Layers for Superconducting Fault Current Limiters under Load Conditions. *IEEE Transactions on Applied Superconductivity*, *29*(8). https://doi.org/10.1109/TASC.2019.2952315

Kim, S. Y., & Kim, J. O. (2011). Reliability evaluation of distribution network with DG considering the reliability of protective devices affected by SFCL. *IEEE Transactions on Applied Superconductivity*, *21*(5), 3561–3569. https://doi.org/10.1109/TASC.2011.2163187

Kulkarni, S., Dixit, M., & Pal, K. (2012). *Study on recovery performance of high T c superconducting tapes for resistive type superconducting fault current limiter applications*. *36*, 1231–1235. https://doi.org/10.1016/j.phpro.2012.06.281

Labos, W., & Grossmann, P. (2014). Case study - 80 kA gas insulated substation Bergen switching station - New Jersey. *Proceedings of the IEEE Power Engineering Society Transmission and Distribution Conference*, 1–5.

Langston, J., Steurer, M., Woodruff, S., Baldwin, T., & Tang, J. (2005). A generic real-time computer simulation model for superconducting fault current limiters and its application in system protection studies. *IEEE Transactions on Applied Superconductivity*, *15*(2 PART II), 2090–2093. https://doi.org/10.1109/TASC.2005.849459

Lee, J., & Joo, S. K. (2013). Economic assessment method for superconducting fault current limiter (SFCL) in fault current-constrained power system operation. *IEEE Transactions on Applied Superconductivity*, *23*(3). https://doi.org/10.1109/TASC.2012.2233540

Lee, S. R., Lee, J. J., Yoon, J., Kang, Y. W., & Hur, J. (2017). Protection Scheme of a 154-kV SFCL Test Transmission Line at the KEPCO Power Testing Center. *IEEE Transactions on Applied Superconductivity*, *27*(4), 2–6. https://doi.org/10.1109/TASC.2017.2669159

Leung, E. M. (2009). Superconducting fault current limiters. *IEEE Power Engineering Review*, *20*(8), 15–18, 30. https://doi.org/10.1109/39.857449

Liang, H., Chen, Y., Duan, R., Lu, Y., & Sheng, J. (2022). Numerical Study on the On-Grid Performance of Superconducting Cable Cooperated with R-SFCL. *IEEE Transactions on Applied Superconductivity*, *32*(4). https://doi.org/10.1109/TASC.2022.3141039

List of Superconductors. (n.d.). https://en.wikipedia.org/wiki/List_of_superconductors

Manohar, P., & Ahmed, W. (2012). Superconducting Fault Current Limiter to Mitigate the Effect of DC Line Fault in VSC-HVDC System. *2012 International Conference on Power, Signals, Controls and Computation*, 1–6. https://doi.org/10.1109/EPSCICON.2012.6175282

Moyzykh, M., Gorbunova, D., Ustyuzhanin, P., Sotnikov, D., Baburin, K., Maklakov, A., Magommedov, E., Shumkov, A., Telnova, A., Shcherbakov, V., Kumarov, D., Sabirov, L., Medovik, M., Kadyrbaev, A., Alexandrov, S., Mikoyan, I., Samoilenkov, S., & Vavilov, A. (2021). First Russian 220 kV superconducting fault current limiter for application in city grid. *IEEE Transactions on Applied Superconductivity*, *August 2017*, 1–7. https://doi.org/10.1109/TASC.2021.3066324

Nagarathna, M. C., H., V. M., & R., and S. (2015). *A Review on Super Conducting Fault Current Limiter (SFCL) in Power System*. *3*(2), 485–489.

Nejra, Č., Avdakovi, S., Hivziefendi, J., & Kobilica, A. (2019). *A new approach for the fault identi fi cation , localization , and classi fi cation in the power system*. *7*(June), 259–280.

Nemdili, S., & Belkhiat, S. (2012). Modeling and simulation of resistive superconducting fault-current limiters. *Journal of Superconductivity and Novel Magnetism*, *25*(7), 2351–2356. https://doi.org/10.1007/s10948-012-1685-z

Okakwu, I. K., Orukpe, P. E., & Ogujor, E. A. (2018). Application of Superconducting Fault Current Limiter (SFCL) in Power Systems: A Review. *European Journal of Engineering Research and Science*, *3*(7), 28. https://doi.org/10.24018/ejers.2018.3.7.799

Qian, K., Guo, Z., Terao, Y., & Ohsaki, H. (2017). Electromagnetic and thermal design of superconducting fault current limiters for DC electric systems using superconducting. *20th International Conference on Electrical Machines and Systems, ICEMS 2017*.

Saha, D., Roy, B. K. S., & Das, P. N. (2019). Online adaptive protection scheme for electrical distribution network with high penetration of renewable energy sources. *Journal of Engineering Research (Kuwait)*, *7*(2), 242–258.

Seyedi, H., & Tabei, B. (2012). Appropriate Placement of Fault Current Limiting Reactors in Different HV Substation Arrangements. *Circuits and Systems*, *03*(03), 252–262. https://doi.org/10.4236/cs.2012.33035

Xue, S., Gao, F., Sun, W., & Li, B. (2015). Protection principle for a DC distribution system with a resistive superconductive fault current limiter. *Energies*, *8*(6), 4839–4852. https://doi.org/10.3390/en8064839

Yılmaz, B., & Gençoğlu, M. T. (2022). Modeling the limiting performance of resistive superconductor fault

current limiters for 2G HTS tape. *Firat University Journal of Experimental and Computational Engineering*, *1*(2), 49–59. https://doi.org/10.5505/fujece.2022.32042

Zampa, A., Holleis, S., Badel, A., Tixador, P., Bernardi, J., & Eisterer, M. (2022). Influence of Local Inhomogeneities in the REBCO Layer on the Mechanism of Quench Onset in 2G HTS Tapes. *IEEE Transactions on Applied Superconductivity*, *32*(3). https://doi.org/10.1109/TASC.2022.3151950

Zenitani, Y., & Akimitsu, J. (2002). Discovery of the new superconductor MgB2 and its recent development. *Oyobuturi*, *71*(1), 17–22. https://doi.org/10.11470/oubutsu1932.71.17

Zhang, J., Teng, Y., Qiu, Q., Jing, L., Zhao, L., Xi, X., Zhou, W., Zhang, D., Zhu, Z., Guo, W., Zhang, G., Lin, L., & Xiao, L. (2019). Fabrication and Tests of a Resistive-Type Superconducting Fault Current Limiter Module Based on Coated Conductors. *Journal of Superconductivity and Novel Magnetism*, *32*(6), 1589–1597. https://doi.org/10.1007/s10948-018-4869-3

Zhang, X., Ruiz, H. S., Zhong, Z., & Coombs, T. A. (2015). *Implementation of Resistive Type Superconducting Fault Current Limiters in Electrical Grids : Performance Analysis and Measuring of Optimal Locations*. *August*.

Zhu, Jiahui, Zhang, H., Chen, P., Zhao, Y., Qin, H., Wei, D., Lu, K., Dong, Y., Zhang, K., & Du, Q. (2020). Experimental investigation of current limiting characteristics for a novel hybrid superconducting fault current limiter (SFCL) with biased magnetic field. *Journal of Physics: Conference Series*, *1559*(1). https://doi.org/10.1088/1742-6596/1559/1/012104

Zhu, Jiahui, Zhao, Y., Chen, P., Jiang, S., Wang, S., Fang, J., Zhao, X., & Wang, H. (2019). Magneto-Thermal Coupling Design and Performance Investigation of a Novel Hybrid Superconducting Fault Current Limiter (SFCL) With Bias Magnetic Field Based on MATLAB / SIMULINK. *IEEE Transactions on Applied Superconductivity*, *29*(2), 1–5. https://doi.org/10.1109/TASC.2019.2892295

Zhu, Jiahui, Zheng, X., Qiu, M., Zhang, Z., Li, J., & Yuan, W. (2015). Application Simulation of a Resistive Type Superconducting Fault Current Limiter (SFCL) in a Transmission and Wind Power System. *Energy Procedia*, *75*, 716–721. https://doi.org/10.1016/j.egypro.2015.07.498

Zhu, Jiamin, Chen, S., & Jin, Z. (2022). Progress on Second-Generation High-Temperature Superconductor Tape Targeting Resistive Fault Current Limiter Application. *Electronics (Switzerland)*, *11*(3). https://doi.org/10.3390/electronics11030297